Accelerated corrosion and repair of reinforced concrete columns using carbon fibre reinforced polymer sheets

C. Lee, J.F. Bonacci, M.D.A. Thomas, M. Maalej, S. Khajehpour, N. Hearn, S. Pantazopoulou, and S. Sheikh

Abstract: An experimental study on the simulation of corrosion in large-scale reinforced concrete columns and their repair using carbon fibre reinforced polymer (CFRP) sheets is presented. Seven columns were subjected to an accelerated corrosion regime, wrapped using CFRP sheets, then tested to structural failure and (or) subjected to further post-repair accelerated corrosion, monitoring, and testing. Accelerated corrosion was achieved by adding sodium chloride to the mixing water, applying a current to the reinforcement cage, and subjecting the specimens to cyclic wetting and drying. Results showed that the CFRP repair greatly improved the strength of the repaired member and retarded the rate of post-repair corrosion. Moreover, subjecting the repaired column to extensive, post-repair corrosion resulted in no loss of strength or stiffness and only a slight reduction in the ductility of the repaired member.

Key words: accelerated corrosion, carbon fibre reinforced polymer, composites, corrosion damage, corrosion rate, external confinement, reinforced concrete columns.

Résumé : Une étude expérimentale de la simulation de la corrosion de colonnes en béton armé à grande échelle et de leur réparation par l'utilisation de feuilles de polymère renforcé de fibres de carbone (PRFC) est présentée. Sept colonnes ont été soumises à un régime accéléré de corrosion, enrobées de feuilles de PRFC, puis ont été testées jusqu'à la défaillance structurale et/ou soumises à une corrosion accélérée additionnelle après réparation, une surveillance et des tests. La corrosion accélérée a été atteinte par l'addition de chlorure de sodium dans l'eau de mélange, l'application d'un courant à la cage de renforcement, et la soumission des spécimens à un cycle d'humidification et de séchage. Les résultats ont montré que les réparations avec le PRFC ont grandement amélioré la résistance du membre réparé et ont retardé le taux de corrosion après réparation. De plus, de soumettre une colonnes réparée à une corrosion intensive après réparation n'a causé aucune perte de résistance ou de rigidité, et n'a résulté qu'en une faible réduction de la ductilité du membre réparé.

Mots clés : corrosion accélérée, polymère renforcé de fibres de carbone, composites, dommages par corrosion, taux de corrosion, coffrage externe, colonnes en béton armé.

[Traduit par la Rédaction]

Introduction

Reinforced concrete infrastructure represents a multi-billion dollar investment in North America, and premature deterioration due to corrosion has become an increasingly significant problem. Transportation structures such as reinforced concrete bridge columns are especially vulnerable to corrosion attack because of their extensive exposure to de-icing salts. Briefly, steel in concrete is protected from corrosion by the natural formation of a passive layer in the highly alkaline (pH > 13) environment that normally prevails in concrete. Chloride ions present in de-icing salts can cause the breakdown of this passive layer and initiate corrosion, provided that the chlorides, oxygen, and moisture are present in sufficient quantities at the level of the reinforcing steel. The effects of corrosion are three-fold: (*i*) it results in the dissolution of steel, causing loss of bar cross section and ductility; (*ii*) it generates expansive corrosion products,

Received August 4, 1999. Revised manuscript accepted March 1, 2000.

C. Lee,[1] J.F. Bonacci,[2] M.D.A. Thomas, M. Maalej,[3] S. Khajehpour,[4] N. Hearn,[5] S. Pantazopoulou,[6] and S. Sheikh. Department of Civil Engineering, University of Toronto, Toronto, ON M5S 1A4, Canada.

Written discussion of this article is welcomed and will be received by the Editor until February 28, 2001.

[1]Current address: Halsall Associates Ltd., 2300 Yonge Street, P.O. Box 2384, Toronto, ON M4P 1E4.
[2]Author to whom all correspondence should be addressed (e-mail: bonacci@civ.utoronto.ca).
[3]Current address: Department of Civil Engineering, National University of Singapore, Singapore 119260.
[4]Current address: Berger Lehman Associates, 411 Theodore Fremd Avenue, Rye, NY 10580, U.S.A.
[5]Current address: Department of Civil and Environmental Engineering, University of Windsor, Windsor, ON N9B 3P4
[6]Current address: Department of Civil Engineering, Demokritus University of Thrace, Xanthi, Greece 67100.

Table 1. Laboratory testing plan.

Column	Accelerated corrosion	Repair	Structural testing	Objective
Control	No	No	Yes	Determine the unconfined column strength
COL1	Yes	No	No	Investigate wet–dry cycling as an alternative accelerated corrosion technique; Observe internal damage through cross-sectional cuts
COL2	No	No	No	Determine natural corrosion rate
COL3	Yes	No	Yes	Determine strength loss due to corrosion; Gravimetric steel loss calculations
COL4	Yes	Yes	No	Determine decrease in corrosion rate provided by the repair
COL5	Yes (×2)	Yes	Yes	Evaluate performance of repair after post-repair corrosion damage
COL6	Yes	Yes	Yes	Determine the strength recovered by repair

causing cracking, spalling, and delamination of the concrete cover; and (*iii*) it causes loss of bond capacity due to concrete damage. The serviceability and, ultimately, the structural capacity of the member is affected.

Traditional repair methods have shown limited success; many are either costly or labour-intensive and often vulnerable to the same deterioration mechanisms as the original structure. As a result, second- and third-generation repairs being performed on the same members have become all too common. As corrosion damage leads to escalating repair costs, the need grows for an innovative repair solution that is durable, cost effective, and most importantly, resistant to corrosion. Advanced composite materials such as fibre reinforced polymers (FRPs) and, more specifically, external confinement using these materials have emerged as a promising new technology for the repair of corroding structures. It is well known that confinement increases the strength and ductility of wrapped or jacketed members (Spoelstra and Monti 1999; Samaan et al. 1998). However, increasing attention in recent years has been given to the advantages confinement can afford corrosion-damaged columns (Pantazopoulou et al. 2000; Neale and Labossière 1998; FRP International 1998).

It is anticipated that the use of FRP wraps for addressing corrosion-related problems will be met by some resistance in the concrete repair industry. Indeed, evidence for this can be found in the following statement from a recent article that otherwise extols the virtues of carbon-fibre reinforcement; the authors state "… carbon-fiber sheet composites should not be used to confine, arrest, or neutralize the effects of corroding reinforcing steel." (Thomas and Kline 1996). Such comments may be justified on the assumption that the simple confinement of an element suffering from reinforcement corrosion merely addresses the symptoms of the distress and not the cause. In other words, neither the environment immediately in the vicinity of the steel nor the electro-potential of the steel are dealt with directly by wrapping the surface of the element with a confining layer. Thus one might expect the corrosion process to continue unabated after completion of the repair. Considering these points in isolation of other factors may well lead to the conclusion that such a repair approach is not appropriate for this type of deterioration. However, this somewhat short-sighted position fails to recognize the potential impact of a number of consequences that arise when an element is confined by externally bonded FRP. These are

- The FRP wrap will act as a low-permeability barrier to further supply of water and oxygen, both of which are required for damaging corrosion to occur.
- The physical confinement may impede the growth of corrosion products and thus stifle the corrosion reaction itself, as suggested by Pantazopoulou et al. (2000) and studied by Hearn and Aiello (1998).
- Provided sufficient external confinement is applied, the mechanical response of the column may not be compromised by further loss of the reinforcement within the confined area.

It is the opinion of the authors that the influence of these factors on the overall long-term performance of FRP-wrapped columns merits further investigation before this promising repair technique is dismissed.

The experimental work presented here is part of a larger on-going project at the University of Toronto under the ISIS (Intelligent Sensing for Innovative Structures) Canada research network. In this study, third-scale models of field columns were corroded under a galvanostatic accelerated corrosion regime, wrapped using carbon fibre reinforced polymer (CFRP) sheets, then tested to structural failure. Specific objectives of the work reported herein included (*i*) establishing optimum laboratory procedures for accelerated corrosion simulation and corrosion monitoring, (*ii*) studying the result of corrosion and repair on the mechanical behaviour of reinforced concrete columns, (*iii*) investigating the effects of the FRP wrap on post-repair corrosion, and (*iv*) evaluating the effects of post-repair corrosion on the structural performance of the repair.

Experimental overview

A total of seven, large-scale, spirally reinforced concrete columns were constructed for the study: five were subjected to an accelerated corrosion regime and three of these were repaired using CFRP sheets (see Table 1 for an overview of the experimental program). The efficacy of the repair was then evaluated by determining (*i*) the post-repair strength and ductility (COL6), (*ii*) the post-repair corrosion rate (COL4), and (*iii*) the performance of the repair after further accelerated corrosion (COL5). COL2 was used to determine the natural corrosion rate of the column in the test environment, and the post-repair corrosion was monitored (COL4) and compared against these values to determine the effect of the repair.

Specimen preparation

The overall dimensions and cross-sectional details are shown in Fig. 1. Specimens were 305 mm in diameter and 1016 mm in height. The clear concrete cover was 20 mm.

Fig. 1. Specimen geometry.

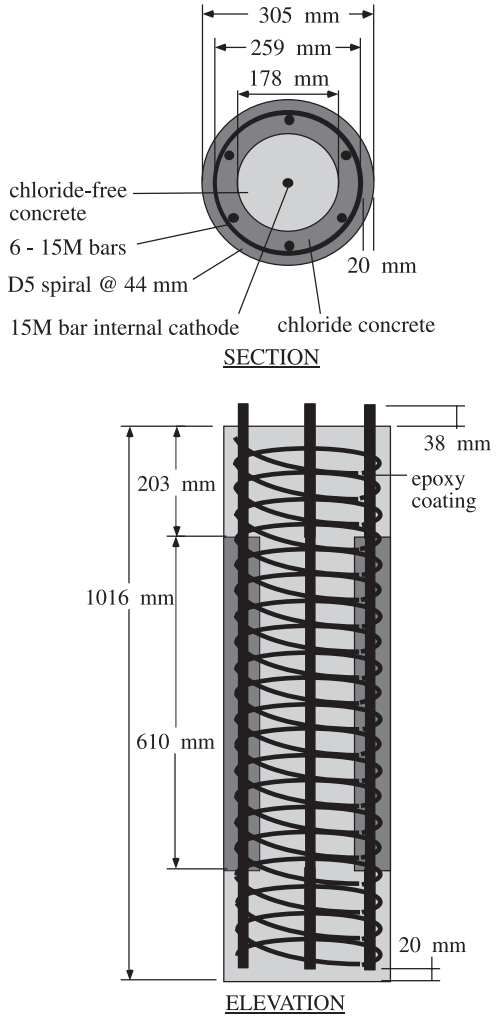

Each column was reinforced with six No. 15 longitudinal reinforcing bars and D5 spiral at 44-mm spacing, providing reinforcement ratios of 1.7% (by area) in the longitudinal direction and 1.1% (by volume) in the transverse direction. A seventh No. 15 bar was placed longitudinally in the centre of the column to serve as an internal cathode for accelerated corrosion testing. To eliminate any end effects, corrosion was discouraged outside the test region by epoxy-coating the upper and lower 203-mm sections of the reinforcement cage. Thus the middle half of the column constituted the effective test region.

Specimens were designed to model aging reinforced concrete bridge columns. To simulate chloride contamination of the cover by de-icing salt spray, two types of concrete were placed simultaneously in each specimen. Chloride-contaminated concrete (achieved by adding 2% chlorides by mass of cement to the mixing water in the form of sodium chloride) was cast around the reinforcement cage to depassivate the steel. Regular, uncontaminated concrete was cast in the core (as well as in the end regions) to establish concentration gradients more accurately modeling field conditions. A high water-to-cement ratio of 0.62 was used to yield a concrete that would facilitate the ingress of oxygen and moisture through the cover. The average 28-day compressive strengths of the regular and chloride-contaminated concrete mixes were 24 and 23 MPa, respectively.

Fig. 2. Accelerated corrosion test setup.

Accelerated corrosion simulation

All columns (except COL2 and the control specimen) were subjected to galvanostatic accelerated corrosion by impressing a current through the reinforcement cage by applying a fixed potential across the anode (reinforcement cage) and the internal cathode. Columns were initially immersed in water up to the bottom of the test region, wrapped in wet burlap, and covered in plastic to maintain a high humidity environment. To investigate wet–dry cycling as an alternative to constant humidity exposure, COL1 was alternately dried then immersed to the upper test region boundary in a 3% NaCl solution. Accelerated corrosion testing began 22 weeks after casting the specimens. Figure 2 shows the accelerated corrosion test setup.

Corrosion current, circumferential expansion, and cracking were monitored throughout the accelerated corrosion period to determine the (*i*) amount of steel loss, (*ii*) extent of damage caused by formation of expansive corrosion products, and (*iii*) pattern of cracking. The amount of steel loss was estimated using Faraday's Law (by integrating the corrosion area under the current vs. time curve) and confirmed in one specimen (COL3) by comparing the weight of the reinforcement cage before and after corrosion. Circumferential expansion of the column was measured by three independent methods: (*i*) using long-gauge Bragg grating fibre optic strain sensors (Fan et al. 1996) mounted 50mm below the mid-height of the column, (*ii*) using mechanical expansion collars (see Fig. 3) mounted 50 mm above the mid-height of the column, and (*iii*) manually summing measured crack widths around the circumference of the column at two sections: at mid-height and at the location of maximum perceived cracking.

The natural corrosion rate of COL2 was monitored by measuring the macro-cell corrosion current between the centrally mounted cathode and the reinforcing cage (anode). This was achieved by electrically connecting the anode and cathode via a 1000 Ω resistor and measuring the drop in potential across the known resistance. Similar measurements were made for COL4 after repair (which was well after accelerated corrosion was terminated). In addition to these

Fig. 3. Mechanical expansion collar.

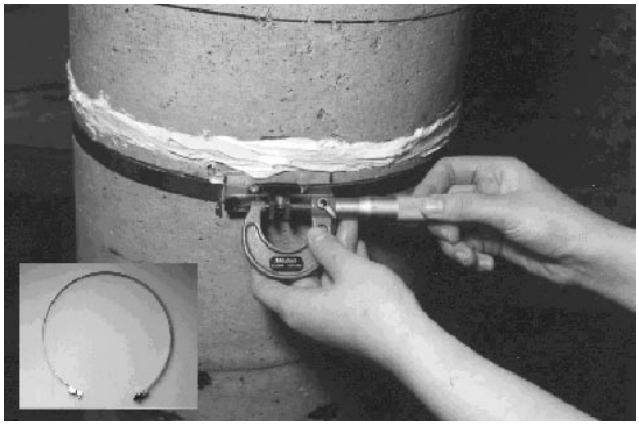

simple measurements, corrosion rates were also determined for COL2 and COL4 using linear polarization techniques. For these tests, one of the longitudinal reinforcing bars was considered to be the working electrode, the centrally mounted cathode was used as the counter electrode, and a standard copper – copper sulphate half-cell placed on the top surface of the column was used as a reference electrode. Measurements were made using a Gamry Instruments CMS100 System using Tafel constants of 52 mV for the passive state and 26 mV for active corrosion, as is recommended by the system supplier.

Repair and structural testing

Pre-impregnated Replark Type 30 CFRP sheets were used in the repair of damaged columns. The specified design thickness of these sheets is 0.167 mm with a tensile strength and elastic modulus of 3400 MPa and 230 GPa, respectively, as reported by the manufacturer. The column surface was sanded, cleaned, and primed as per the manufacturer's specifications and the CFRP sheets were applied in two continuous layers with a 100-mm overlap. Long-gauge Bragg grating fibre optic sensors were integrated into the repair at mid-height.

Designated columns (see Table 1) were tested to failure in monotonic, uniaxial compression under load control in the University of Toronto's Baldwin machine with an ultimate capacity of 1.2 million pounds. The loading head was fitted with a spherical seat. To force the failure within the test region, additional confinement was provided outside the test region by 9.5-mm thick steel end collars. Instrumentation included four linear variable differential transformers (LVDTs) placed 90° apart to measure axial deformation over a gauge length of 565 mm (see Fig. 4). A fifth LVDT was placed under the loading head to measure its displacement. Electrical strain gauges (50-mm length) were installed at mid-height on COL1 and on the outside of the CFRP wrap on COL6 to measure circumferential strain. Circumferential strain in COL6 was also monitored simultaneously using the embedded fibre optic sensors.

Results of study

Accelerated corrosion simulation

Five specimens underwent accelerated corrosion for a total of 49 weeks, at which time specimens reached an average

Fig. 4. Structural test setup.

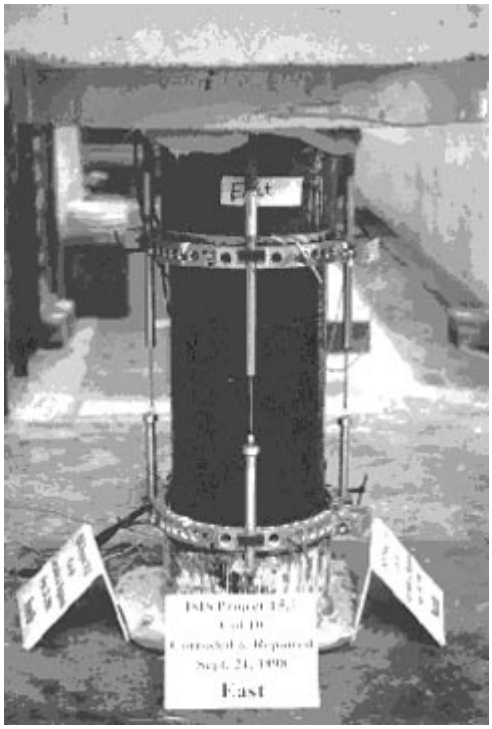

expansion of 0.3%. Steel loss estimates (derived from the corrosion current data) and the extent of cracking (determined from visual inspection) were used as the primary indicators of damage. At the end of the first accelerated corrosion simulation, the estimated maximum steel loss in the columns ranged from 7 to 10%. Hammer-sounding surveys revealed isolated locations of cover delamination. Average maximum circumferential strains ranged from 0.002 to 0.003. One specimen (COL5) was subjected to further accelerated corrosion after repair to evaluate the effect of the repair on corrosion rates. The resulting damage in the specimens is summarized in Table 2.

Corrosion of the specimens proceeded much slower than anticipated with virtually no damage observed in the first half of the corrosion run. Therefore, several changes were made to the accelerated corrosion regime to increase the rate of corrosion:

- The lengths of the wetting and drying cycles were varied throughout the experiment to establish the optimum cycle (i.e., that which produced the greatest damage). This was done empirically by varying the cycle frequency and the ratio of the durations of the wet and dry periods and observing (*i*) changes to the corrosion current levels, (*ii*) the apparent moisture levels in the concrete surface, and (*iii*) formation of new cracks. After a number of trials, a cycle of 1 day wet, 2.5 days dry was found to be most effective in causing damage.
- All columns were subjected to wet–dry cycling after approximately 25 weeks of the corrosion testing once it was determined that this was more effective in producing damage than constant humidity exposure.
- At 28 weeks, the voltage on one specimen was increased from the initial 6 V setting to 12 V to observe the effects of increasing voltage on accelerating damage. When fa-

Table 2. Summary of accelerated corrosion results.

Specimen	Steel loss (%)	Ave. circumferential strain[a] ($\times 10^{-3}$)
COL1	6.7	1.8
COL3	7.5	1.6
COL4	7.8	1.8
COL5	9.5	1.6
COL5[b]	8.5	1.6
COL6	9.3	2.1

[a]Average circumferential strain as measured by mechanical expansion collars.
[b]Post-repair accelerated corrosion.

vourable results were obtained, at 33 weeks the voltage on all columns was raised to 12 V.

Dramatic increases in the rate of expansion per unit of steel loss were experienced by all specimens after the changes discussed above were implemented (see COL5 in Fig. 5). The lack of damage indicated in the early part of the accelerated corrosion for COL5 was likely due to the lack of oxygen resulting from the maintenance of constant relative humidity. Subsequent series of columns (as represented by COLS6 in Fig. 5) were exposed to this modified accelerated corrosion regime from the onset and similar high rates of damage were observed from the beginning of the accelerated corrosion testing period.

Although an effort was made to implement changes to the regime in such a manner that the effects of each change could be assessed independently, this was not always possible. Therefore, it is not possible to determine with certainty which change triggered the acceleration of damage. A cursory examination of the corrosion current and expansion data suggests that the increase in voltage had the greatest effect on accelerating circumferential expansion.

In addition, two key factors were missing from this accelerated corrosion regime. First, specimens were corroded in a climate-controlled laboratory, with relatively constant ambient temperature and humidity and, therefore, not exposed to deleterious environmental conditions such as temperature fluctuations, freezing and thawing, etc. Second, though columns in the field are almost always subjected to considerable dead and live loads, specimens in this test remained unloaded throughout the corrosion run.

Moreover, although a significant current was applied, the anodic area was large (six longitudinal bars plus spiral reinforcement) compared with the cathode. Thus, the resulting anodic current density, as well as the cathode-to-anode ratio, was very low. In general, the rate of corrosion would be expected to be higher when the area of the cathode is increased with respect to the anode.

Perhaps the greatest problem, however, was the cathode placement and configuration. The use of a centrally located cathode resulted in a large distance between the anode and cathode, as well as a very large cover depth to the cathode (the use of an internally located cathode was necessary in this study to facilitate post-repair corrosion). The spacing of the electrodes is significant because ions must travel from one electrode to the other to complete the electrochemical circuit. The spacing between the electrodes in this case was likely prohibitively high. Furthermore, the central placement

Fig. 5. Effect of changes to the accelerated corrosion regime on the rate of expansion.

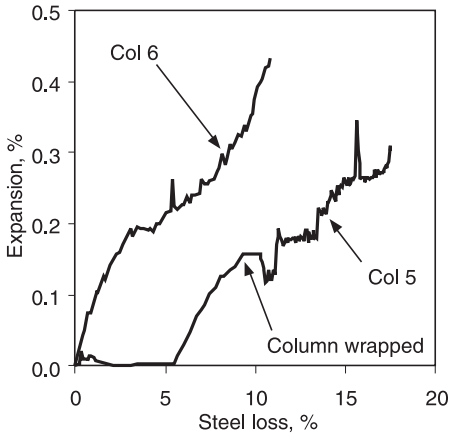

of the cathode meant that oxygen had to diffuse nearly 150 mm to reach the reactive site, and oxygen availability at the cathode is often the rate-determining step in many corrosion reactions. As an aside, subsequent series of columns in this on-going research program were cast with a stainless steel, hollow, perforated pipe as the internal cathode to increase oxygen availability at the cathodic site.

Finally, the expansion data obtained for COL1 suggests that all columns would have benefited from wet–dry cycling from the beginning. In addition, the greatest extent of cracking was observed just above the water level set for the wet phase of the wet–dry cycles. It was reasoned that damage could be induced in a more distributed fashion by varying the water level with each cycle.

Internal observation of corrosion damage

Cross-sectional cuts were taken of COL1 to observe the internal damage, including the extent of cracking and the location, nature, and quantity of the corrosion products formed. A typical cross section (see Fig. 6) showed perfectly delaminated concrete cover (i.e., a single crack formed a continuous ring around the spiral) with radial cracks originating from every longitudinal bar. Because of the close spacing and relatively uniform corrosion of the spirals, very little horizontal cracking occurred in the cover. Thus delaminated cover segments were essentially as tall as the full test region, making it unlikely for spalling to occur. A closer examination of the corrosion damage was also made possible as the reinforcement cage from COL3 was being cleaned for gravimetric steel loss calculation (G1-90-1994). Several interesting observations were recorded:

- The longitudinal bars showed evidence of corrosion damage that was not evident from the cross-sectional cuts. In some areas, the damage was severe, with sections of the steel (especially near the upper test region boundary) resembling a honeycomb.
- Corrosion damage in the spirals was most extensive on the top face of the steel. Severe pitting in certain locations reduced the cross sectional area by more than half.
- In general, the corrosion products were powdery and loosely bonded to the surface of the rebars. These products were red to dark-red in colour and easily removed using the chemical procedure outlined in the ASTM

Fig. 6. Schematic of internal damage as seen from cross-sectional cuts.

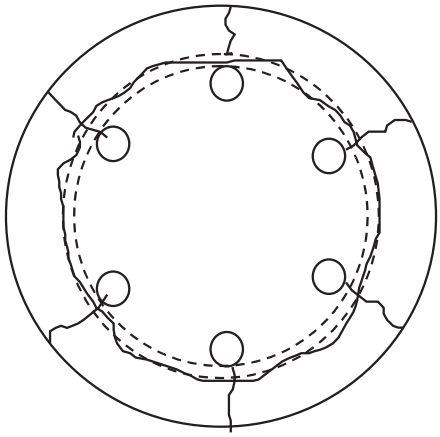

standard (ASTM G1-90-1994). In some locations, however, the corrosion products were so tightly adhered to the reinforcing bars that they could not be removed, even after scraping with a screwdriver. The colour of these products was much darker.

Effect of confinement on post-repair corrosion

Figure 7 shows the half-cell potentials for the reinforcing bars in COL2 and COL4 measured against a copper – copper sulphate standard half-cell during the last 3 weeks of the testing period. Both potentials indicate an active state of corrosion in the reinforcing bars. It is interesting that the steel in COL4 (the repaired column) has a higher negative potential indicating a greater risk of corrosion. This may be due to a higher chloride content at the steel in COL4, owing to the migration of chloride ions to the anode during the accelerated corrosion process. Despite the higher potential of the steel in COL4, the results of linear polarization tests shown in Fig. 8 indicate a significantly lower corrosion current, I_{corr}, in this specimen. Indeed, the value of I_{corr} measured in COL4 was about one half of the current determined for COL2. No attempt was made to determine the corrosion current density because of uncertainty in establishing the anodic area.

The results of macro-cell corrosion currents measured during the same period also indicate significantly lower corrosion rates in COL4. Currents in the range of 0.05 mA were measured between the reinforcing bars and the centrally mounted cathode in COL4 compared with values in the region of 0.09–0.10 mA for COL2.

The reduced corrosion rate observed in the repaired column may be explained solely on the basis of reduced water availability due to the wrap on COL4 (the same wetting and drying regime was used for both specimens). A lower internal moisture content in the concrete will result in a lower electrical conductivity (or higher resistivity), which would be expected to retard the electrochemical corrosion process. The higher resistivity for COL4 is also consistent with observations made for COL5 during accelerated corrosion before and after repair for which the same potential difference of 12 V was used to drive the corrosion reaction. Current after repair in COL5 was generally about 50% lower than that

Fig. 7. Effect of repair on corrosion potentials.

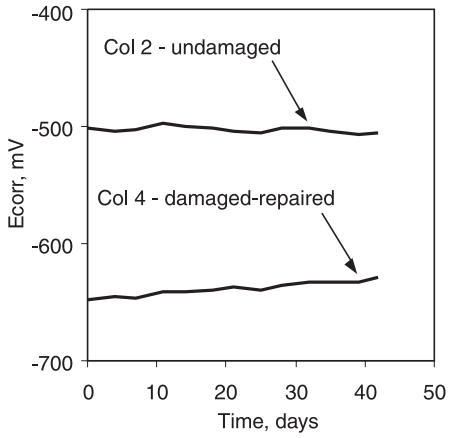

Fig. 8. Effect of repair on corrosion rates.

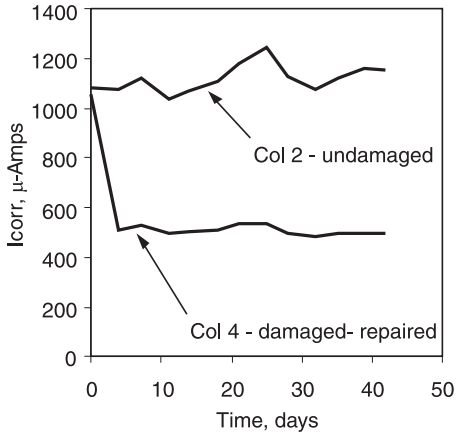

achieved in the unrepaired column. Other factors, such as reduced oxygen availability and physical restraint to the growth of corrosion products, may have also contributed to the lower corrosion.

Structural performance

Discussion of structural testing

The load – axial deformation curves for the four columns tested to structural failure are shown in Fig. 9. Table 3 compares the strength and deformation capacities of the same columns. For the ductility ratio, the yield point was defined by the intersection of two characteristic lines. The first line is a secant slope for the overall load-deformation passing through the curve at 65% of ultimate load, and the second line was constant at the ultimate load value (Sheikh et al. 1997).

Effect of corrosion on structural capacity

Corrosion damage reduced the ultimate load-carrying capacity of the column by 7% with respect to the control specimen. Of more significant note, however, is that the axial deformation at failure was significantly reduced. This column (COL3) failed explosively after initiation of cracking, with virtually no visual or audible warning signs. Displace-

Table 3. Summary of structural test results.

Specimen	Ultimate load (kN)	Axial deformation (mm) and [%] @ Ultimate	Axial deformation (mm) and [%] @ Failure	Ductility ratio
Control	2958	1.4 [0.2]	8.1 [1.4]	9.9
COL3 (corroded, unrepaired)	2762	1.2 [0.2]	2.1 [0.4]	2.7
COL5 (corroded, repaired, corroded)	3659	6.1 [1.1]	9.6 [1.7]	5.1
COL6 (corroded, repaired)	3547	8.2 [1.5]	10.1 [1.8]	7.5

Fig. 9. Load–deformation curves.

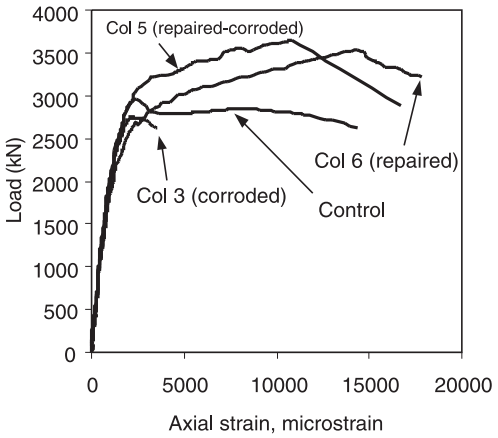

Fig. 10. Load – circumferential strain response.

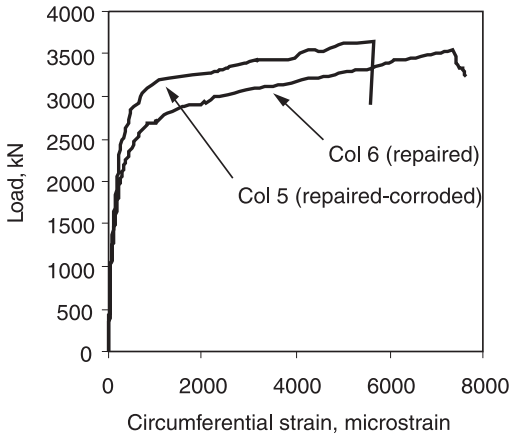

ment data obtained from the LVDTs showed signs of eccentricity in the column response that can be attributed to asymmetric deterioration of the reinforcement. Examination of the reinforcement cage after testing revealed buckling of the longitudinal reinforcement and severe pitting corrosion causing fractures in the spiral reinforcement at 15 locations.

Effect of repair on structural capacity

A considerable improvement in strength was realized in the repaired member (COL6). External confinement increased the load-carrying capacity of the corrosion-damaged column by 28%, exceeding even the load carried by the undamaged control specimen. Behaviour of the wrapped column was also significantly more ductile. Axial deformation at ultimate load was more than six times that of the control and damaged column, and greater energy was required to fail this column (as indicated by the relative areas under the load–displacement curves).

Analysis of the circumferential strain data for both COL5 and COL6 showed that the CFRP wraps were effective in restraining the expansion of the columns with delaminated cover and severely notched spiral transverse reinforcement. Expansion of the sheets progressed at a slow, steady rate. By comparison, the control column experienced a sudden increase in the rate of lateral deformation, increasing nearly exponentially.

Effect of post-repair corrosion on structural capacity

Further exposure to accelerated corrosion following repair resulted in no degradation in the structural capacity of the repaired column despite doubling of the steel loss (see Table 2). In fact, the ultimate load carried by the repaired-then-corroded column (COL5) exceeded even the ultimate load of the repaired-only column (COL6). Measurements taken during accelerated corrosion of COL5 after repair indicated an increment of 0.16% circumferential expansion imposed on the wrapped column. It is likely that a state of active radial confinement would result from the restraint of the CFRP wrap, and this would contribute to increased axial capacity. This prestrain due to corrosion can be observed as well in the load vs. circumferential strain data (Fig. 10) recorded during structural tests of COL5 and COL6. The difference in wrap strain at rupture is of the same order as the strain induced by post-repair corrosion. Axial deformation of COL5 at failure, though somewhat reduced, was still more than 1%. The results for COL5 clearly show that the significant post-repair corrosion damage did not prevent the repaired member from performing well structurally.

Conclusions

The repair of corrosion-damaged columns using CFRP sheets was shown to have the following benefits:

(1) It greatly improved the strength and ductility of the corroded member, increasing the load-carrying capacity of the corroded column by 28%.
(2) It impeded post-repair corrosion, resulting in a 50% decrease in the rate of corrosion after wrapping and a similar decrease in the natural corrosion currents.
(3) Even when subjected to significant post-repair corrosion, the structural performance of the repair system was not compromised.

With respect to simulation of accelerated corrosion, the following accelerated corrosion regime was determined to be optimum in producing damage for this specimen geometry and testing conditions: (*i*) 2% chlorides added to the mixing

water (by weight of cement), (*ii*) 12 V applied to the reinforcement cage, and (*iii*) exposure to wetting and drying cycles of 1 day wet, 2.5 days dry. Cyclic wetting and drying was found to be more effective in producing damage than constant humidity exposure, with cracking most prevalent in the region near the water level of the wet cycle. The selected changes implemented during the accelerated corrosion simulation caused dramatic increases in relationship between expansion and steel loss.

The above conclusions are based on a limited data set; additional laboratory and field studies will provide more data on the longer-term effects of wrapping on the corrosion process, which is needed before the technique becomes generally accepted.

Acknowledgements

Research reported in this article was conducted as part of the ISIS Canada (Intelligent Sensing for Innovative Structures) Network within the federal Network of Centres of Excellence (NCE) program. The funding and support of the NCE program and of the Natural Sciences and Engineering Research Council (NSERC) are gratefully acknowledged. The authors gratefully acknowledge the collaboration and technical assistance of the University of Toronto Institute for Aerospace Studies (UTIAS) Fibre Optic Sensing (FOS) Laboratory under the direction of Dr. R. Tennyson. P. Mulvihill, G. Duck, and G. Manuelpillai were particularly helpful in this regard.

References

ASTM. 1994. Standard practice for preparing cleaning and evaluating corrosion test specimens (ASTM G1-90-1994). *In* Annual Book of ASTM Standards. Vol. 03.02. American Society for Testing and Materials, Philadelphia, Pa., pp. 25–31.

FRP International. 1998. Column repair: Repair of Interstate Highway 40 in Oklahoma City. FRP International, **6**(2): 5.

Fan, N.Y., Maaskant, R., Huang, S., Measures, R.M., and Pantazopoulou, S. 1996. Fiber optic strain sensor or arbitrary gauge length. *In* Advanced composite materials in bridges and structures. *Edited by* M. El-Badry. Canadian Society for Civil Engineering, pp. 999–1009.

Hearn, N., and Aiello, J. 1998. Effect of mechanical restraint on the rate of corrosion in concrete. Canadian Journal of Civil Engineering, **24**: 81–88.

Neale, K.W., and Labossière, P. 1998. Fiber composite sheets in cold climate rehab. Concrete International, **20**(6): 22–24.

Pantazopoulou, S.J., Bonacci, J.F. Sheikh, S., Thomas M.D.A., and Hearn N. 2000. Repair of corrosion damaged columns with FRP wraps. ASCE Journal of Composites in Construction. In press.

Sheikh, S., Pantazopoulou, S., Bonacci, J.F., Thomas, M.D.A., and Hearn, N. 1997. Repair of delaminated circular pier columns by ACM. Ontario Joint Transportation Research Report, Ministry of Transportation Ontario, Toronto, Ont.

Samaan, M., Mirmiran, A., and Shahawy, M. 1998. Model of concrete confined by fiber composites. ASCE Journal of Structural Engineering, **124:** 1025–1031.

Spoelstra, M., and Monti, G. 1999. FRP-confined concrete model, ASCE Journal of Composites for Construction, **3**(3): 143–150.

Thomas, J., and Kline, T. 1996. Strengthening concrete with carbon-fiber reinforcement. Concrete Repair Digest, April/May: 88–92.